

Supporting Information

Improve Charge Injection of the Edge Aligned MoS₂/MoO₂ Hybrid Nanosheets for Highly Robust and Efficient Electrocatalysis of H₂ Production

Shuaishuai Li,^a Li Zhao,^a Shulai Lei,^b Aiping Liu,^{*,a} Jun Chen,^c Chaorong Li,^a Huaping Wu,^d and Liangxu Lin^{*,c,e}

^aCenter for Optoelectronics Materials and Devices, Key Laboratory of Optical Field Manipulation of Zhejiang Province, Zhejiang Sci-Tech University, Hangzhou 310018, China

^bHubei Key Laboratory of Low Dimensional Optoelectronic Materials and Devices, Hubei University of Arts and Science, Xiangyang, 441053 Hubei, China

^cARC Centre of Excellence for Electromaterials Science, Intelligent Polymer Research Institute, Australia Institute for Innovative Materials (AIIM), Innovation Campus, University of Wollongong, Wollongong 2522, Australia

^dKey Laboratory of E&M (Zhejiang University of Technology), Ministry of Education & Zhejiang Province, Hangzhou 310014, China

^eThe State Key Laboratory of Refractories and Metallurgy, and the Institute of Advanced Materials and Nanotechnology, Wuhan University of Science and Technology, Wuhan 430081, China

Table of content:

Figure S1-Figure S12, Table S1

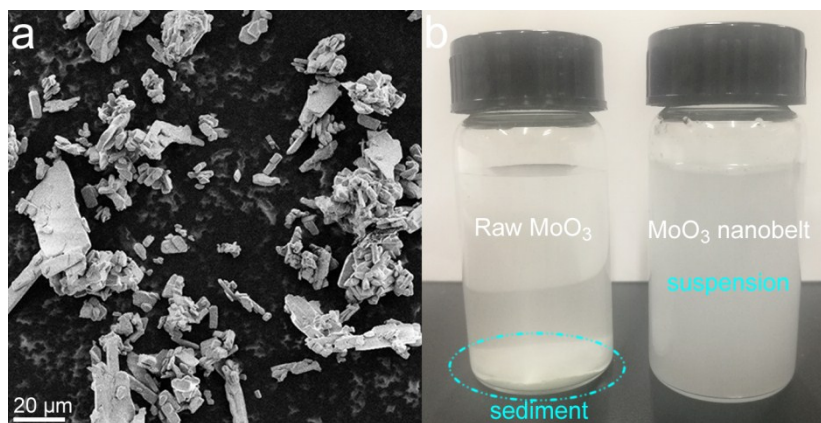


Fig. S1 (a) SEM image of the raw MoO_3 material; (b) Photographs of the suspension of the raw MoO_3 material and MoO_3 nanobelts. The raw MoO_3 material cannot be dispersed well in the aqueous solution, *i.e.* sediment formed with seconds. By contrast, the MoO_3 nanobelt can be dispersed well and stable (no visible sediment formed in half hour) in the aqueous solution, likely owing to the small size.

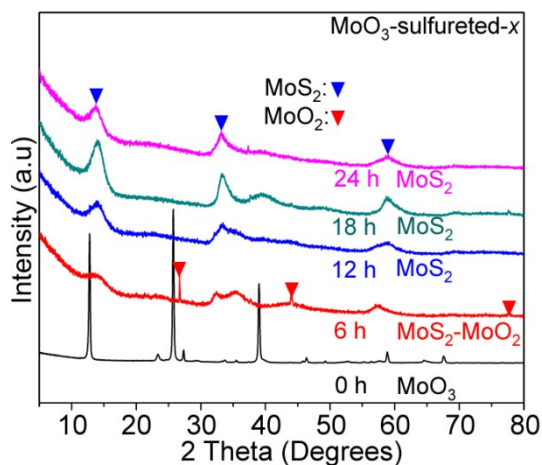


Fig. S2 XRD patterns of the MoO_3 nanobelts (orthorhombic α - MoO_3 , ICDD card: 05-0508) and MoO_3 -sulfured- x samples ($x = 6, 12, 18, 24$ h). Diffraction peaks at 13.9° , 33.4° , and 58.9° are attributed from the (002), (100) and (110) crystal planes of 2H- MoS_2 (ICDD card: 87-2416). Diffraction peaks at around 26.7° , 44.1° , and 77.7° can be ascribed to the metallic monoclinic MoO_2 phase (ICDD card: 32-0671).

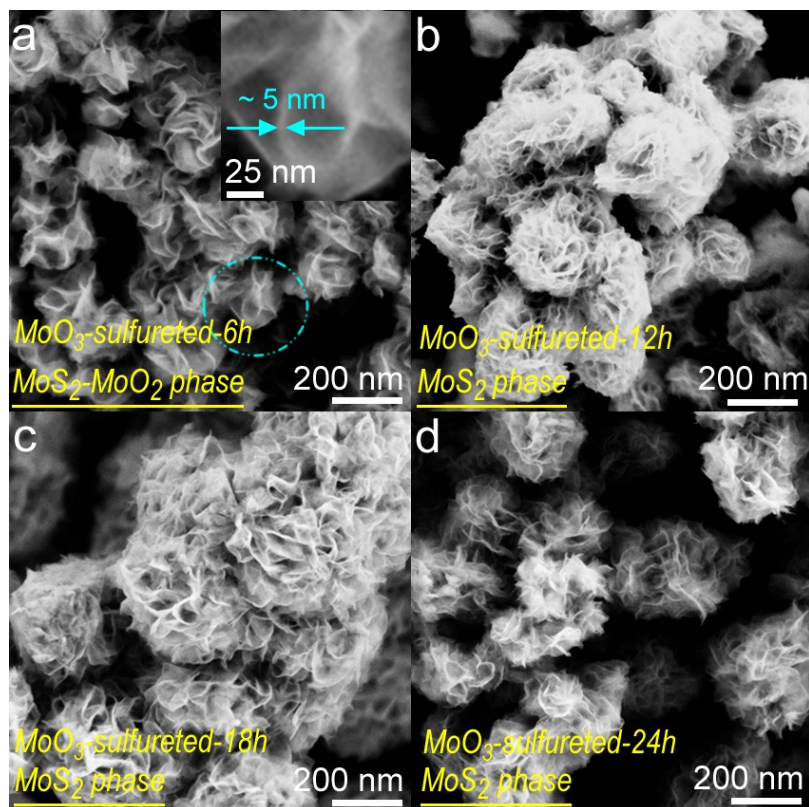


Fig. S3 SEM images of MoO₃-sulfured-6h (MoS₂-MoO₂ composite) (a), MoO₃-sulfured-12h (pure MoS₂) (b) MoO₃-sulfured-18h (pure MoS₂) (c) and MoO₃-sulfured-24h (pure MoS₂) (d). Inset in figure a is the magnified local area (as labeled).

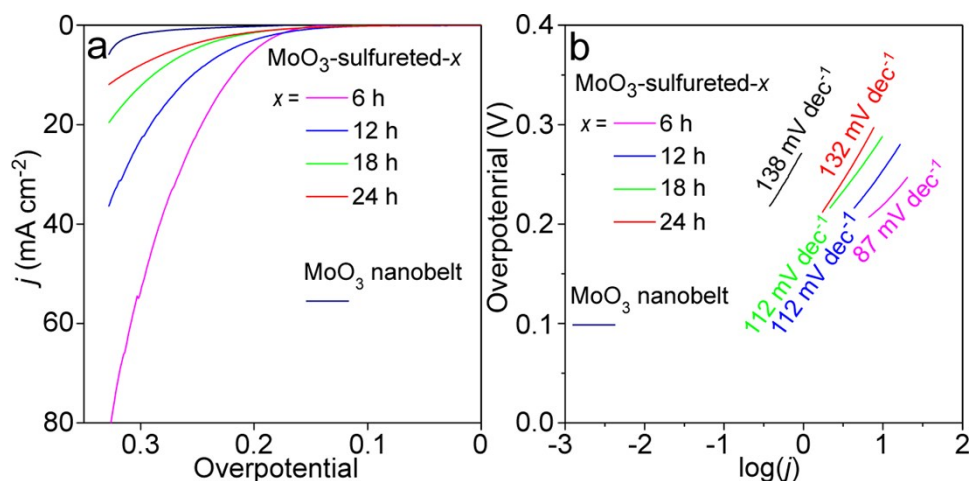


Fig. S4 LSV (a) and Tafel (b) of MoO₃-sulfured-*x* (*x* = 6, 12, 18, 24 h) and MoO₃ nanobelt. The MoO₃-sulfured-6h exhibited the best catalytic performance among these investigated samples.

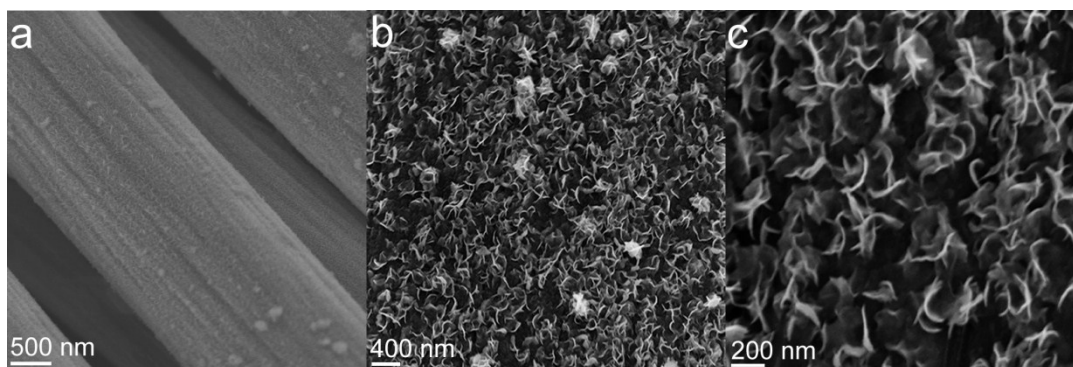


Fig. S5 SEM images of $\text{MoS}_2@\text{MoO}_2/\text{CC}-6\text{h}$.

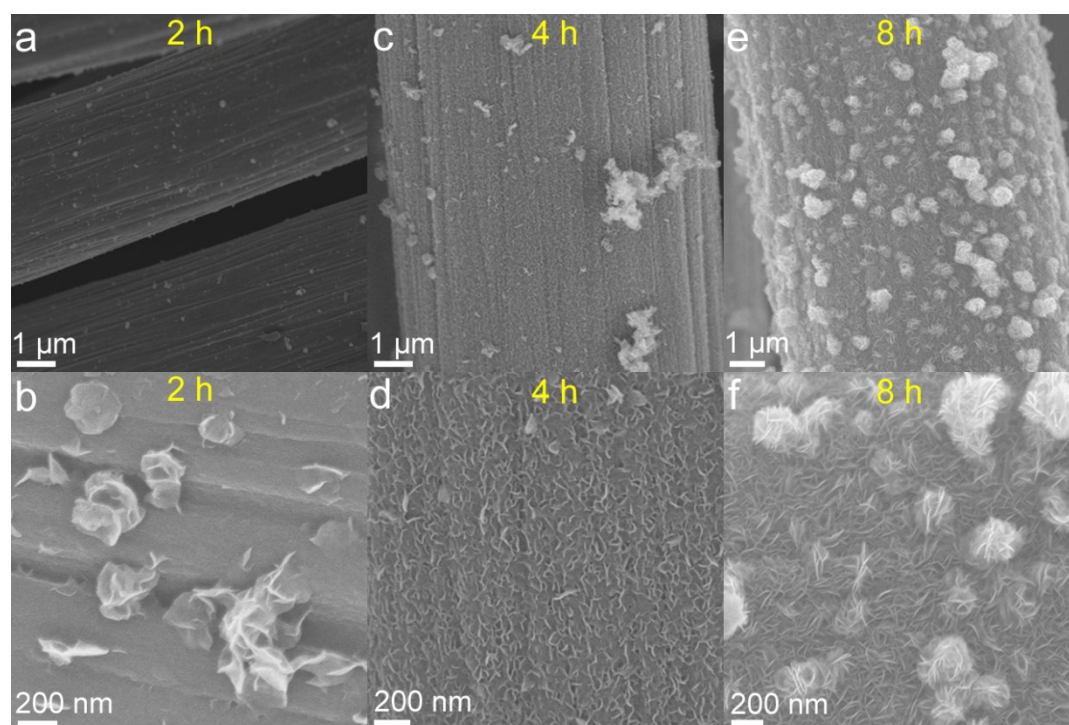


Fig. S6 SEM images of $\text{MoS}_2@\text{MoO}_2/\text{CC}-x$ obtained with different reaction time. a-b) 2h. c-d) 4h. e-f) 8h. In $\text{MoS}_2@\text{MoO}_2/\text{CC}-2\text{h}$, the particle on the surface are really few. Figure b shows some particles found occasionally.

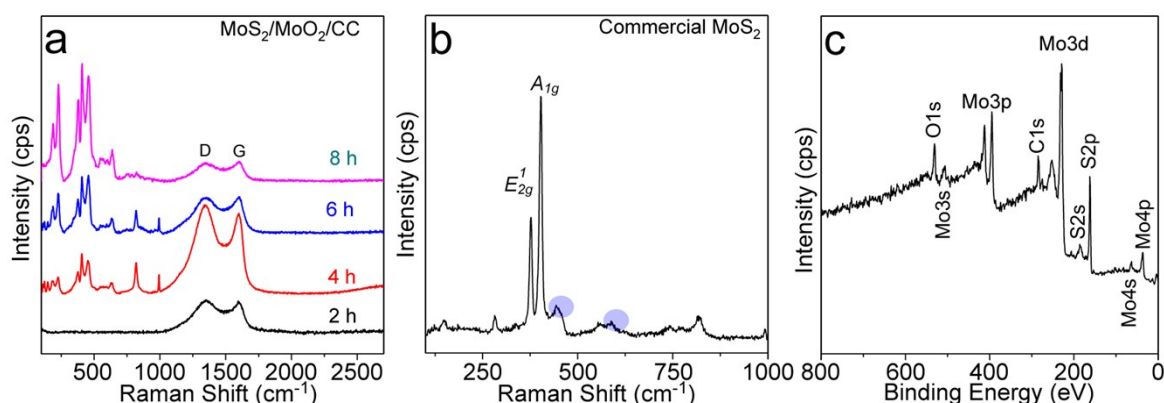


Fig. S7 (a) Raman spectra of $\text{MoS}_2@\text{MoO}_2/\text{CC}-2\text{h}$, $\text{MoS}_2@\text{MoO}_2/\text{CC}-4\text{h}$, $\text{MoS}_2@\text{MoO}_2/\text{CC}-6\text{h}$ and $\text{MoS}_2@\text{MoO}_2/\text{CC}-8\text{h}$; (b) Raman spectrum of the commercial MoS_2 flakes (Sigma-Aldrich, product No: 234842). The highlighted peaks are around 457 and 590 cm^{-1} which were also found in our prepared samples; (c) XPS full survey of the $\text{MoS}_2@\text{MoO}_2/\text{CC}-6\text{h}$.

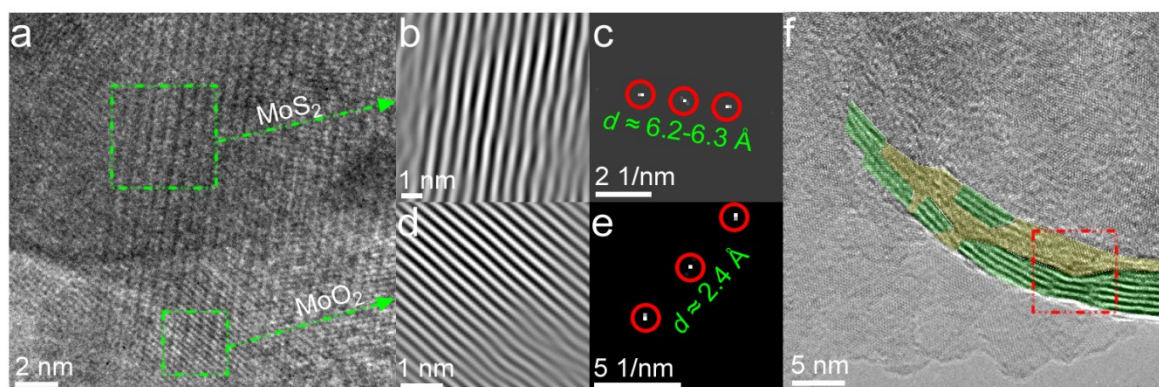


Fig. S8 (a-f) HRTEM image of one sheet show both the 2H-MoS₂ and monoclinic MoO₂ crystal domains (a), which are highlighted as the corresponding simulated HRTEM images (b, d) and FFT patterns (c, e); f) One edge composed by the MoO₂ and MoS₂, with selected area magnified in Fig. 3l.

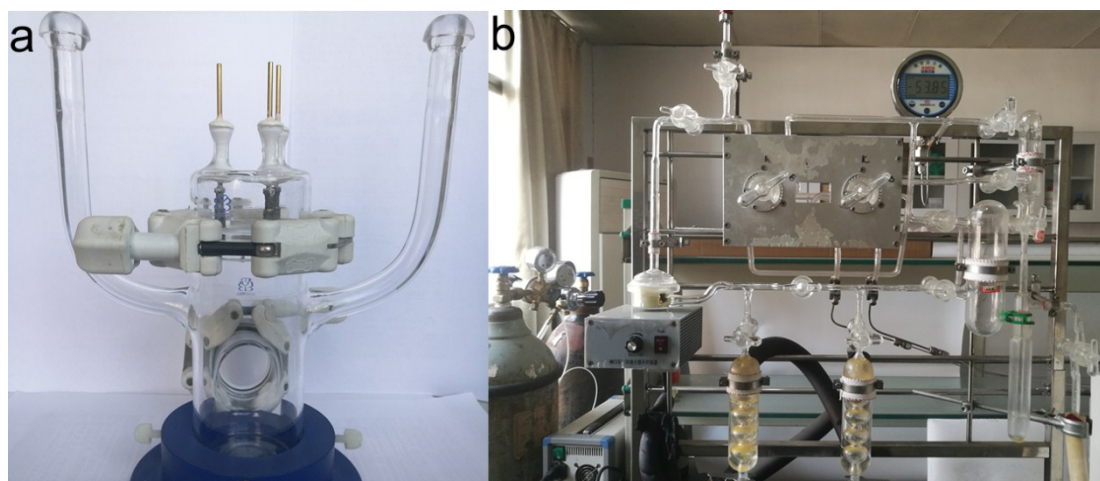


Fig. S9 (a) the photograph of the sealable three-electrode cell for the evaluation of the Faradaic efficiency. In this case, the reference electrode of the Ag/AgCl with saturated KCl was used; (b) The photograph of the full set up used for the estimation of the Faradaic efficiency.

Table S1 Theoretical H₂ production *versus* experimental measured H₂ amount, and Faradaic efficiencies at different period for MoS₂@MoO₂-CC-6h (constant j of 30 mA cm⁻², 1.0 × 1.0 cm² electrode).

Time (min)	20	40	60	80	100	120
Calculated (mmol)	0.1866	0.3732	0.5598	0.7464	0.933	1.116
Measured (mmol)	0.1824	0.3671	0.5516	0.7396	0.9294	1.1105
Faradaic efficiency	97.7%	98.3%	98.5%	99.1%	99.6%	99.2%
Average	98.7%					

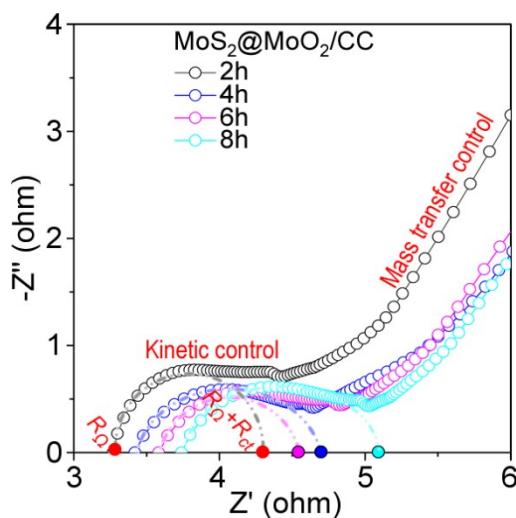


Fig. S10 EIS Nyquist plots of various catalysts modified electrodes in a 0.5 M H_2SO_4 solution at 5 mV s^{-1} . The (R_Ω , $R_\Omega + R_{ct}$) of $\text{MoS}_2@\text{MoO}_2/\text{CC}$ -2h, $\text{MoS}_2@\text{MoO}_2/\text{CC}$ -4h, $\text{MoS}_2@\text{MoO}_2/\text{CC}$ -6h, $\text{MoS}_2@\text{MoO}_2/\text{CC}$ -8h are (3.27Ω , 4.30Ω), (3.42Ω , 4.69Ω), (3.58Ω , 4.54Ω) and (3.74Ω , 5.10Ω), respectively.

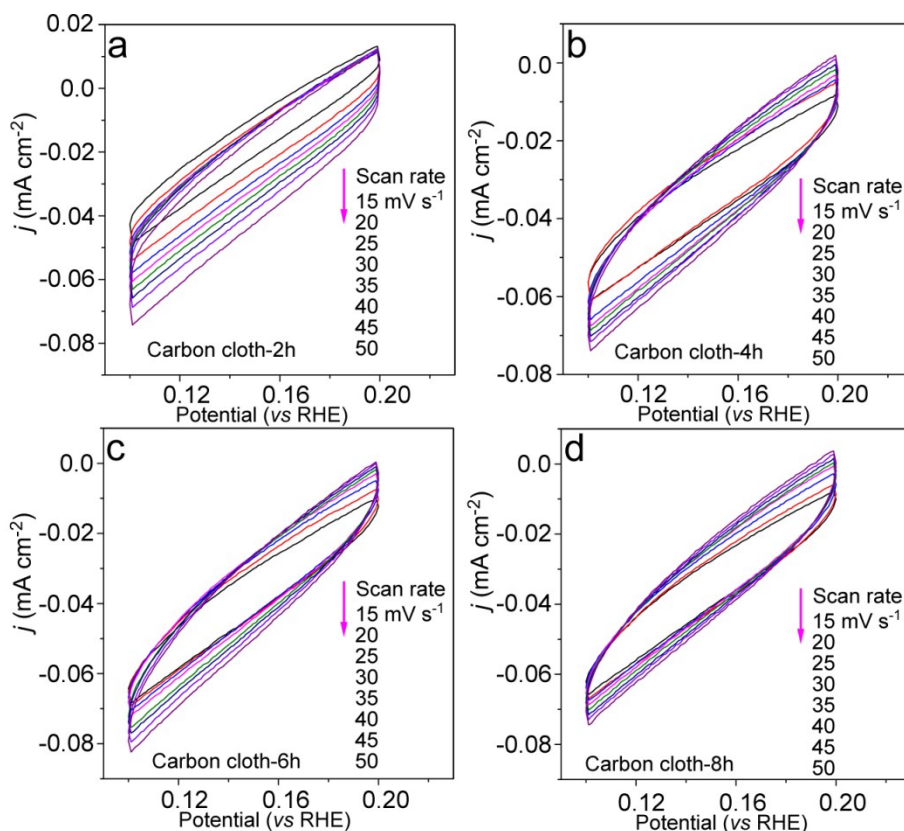


Fig. S11 CV curves of carbon cloth after solvothermal reactions with different reaction time: (a) carbon cloth-2h; (b) carbon cloth-4h; (c) carbon cloth-6h; (d) carbon cloth-8h. The C_{dl} calculated at the potential of 0.15 V of these four samples are nearly identical.

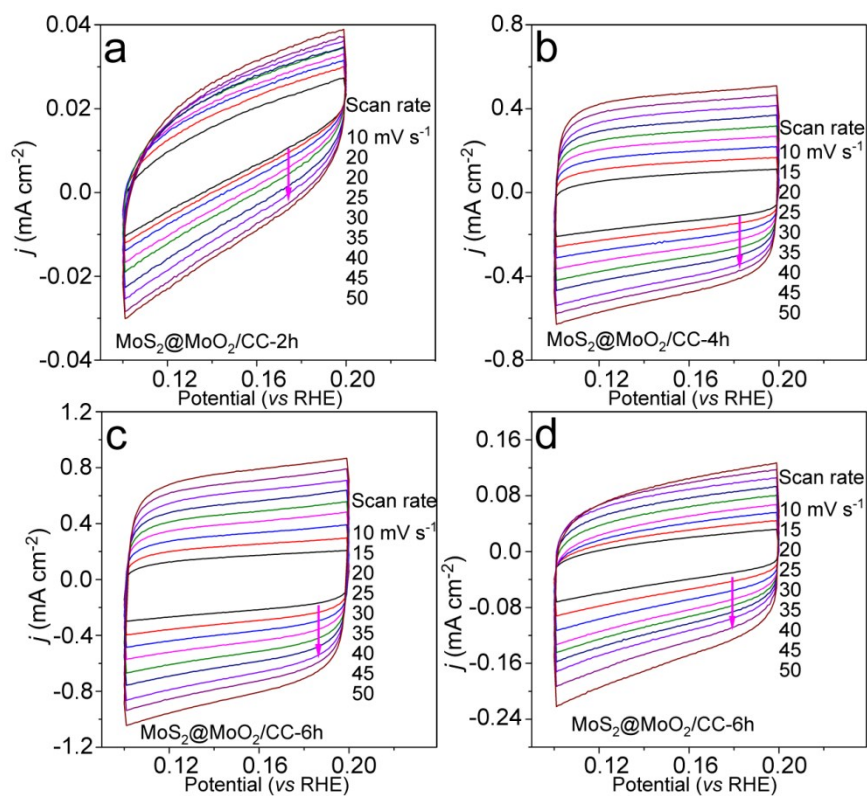


Fig. S12 CV curves of different samples: (a) $\text{MoS}_2@\text{MoO}_2/\text{CC-2h}$; (b) $\text{MoS}_2@\text{MoO}_2/\text{CC-4h}$; (c) $\text{MoS}_2@\text{MoO}_2/\text{CC-6h}$; (d) $\text{MoS}_2@\text{MoO}_2/\text{CC-8h}$.